CHALLENGES IN EUROPEAN AEROSPACE
5TH CEAS AIR & SPACE CONFERENCE

CEAS

Preliminary Design Rules for Electromechanical Actuation Systems – Effects of Saturation and Compliances

Jian FU, Ion HAZYUK, Jean-Charles MARÉ

Institut Clément Ader, INSA-Toulouse, Université de Toulouse
135 Avenue du Rangueil, 31077, Toulouse Cedex 4, France
jian.fu@insa-toulouse.fr, ion.hazyuk@insa-toulouse.fr, jean-charles.mare@insa-toulouse.fr

ABSTRACT

Electromechanical actuator (EMA) is a type of power-by-wire (PBW) actuator that is becoming widely implemented in aerospace industry. Given the application area, designing an EMA is highly constrained in weight, integration space, maintenance costs, dynamic performances, reliability, etc. In order to reduce the EMA's design time, cost and effort, all these constraints should be considered in the preliminary design stages. The problem is that at such early design stages, system engineers need simple and explicit models. Thus, this communication is attempting to formulate simple relations that account for torque and velocity saturation of the EMA as well as compliances effects on its dynamic performance. The simple and parametric models predict the main impact of the sizing variables on performance.

Keywords: Aerospace, EMA, Flight Control, Preliminary Design, Modeling and Simulation

ABBREVIATIONS

F_e , F_{ex}	EMA out and aerodynamic action force	[*N*]
I_s , I_m	DC supplied and motor current	[*A*]
J_m	Inertia of the rotor	[$kg{\cdot}m^2$]
K_p	Position controller gain	[*Nm/m*]
K'_p	Position controller gain for speed limit control architecture	[(*rad/s*)/*m*]
K_v , K'_v	Classical and speed limited architecture velocity controller gain	[*Nm/(rad/s)*]
k_a , k_s , k_t , k_z	Anchorage, nut-screw, transmission and structural compliance	[*N/m*]
k_e	EMA equivalent compliance	[*N/m*]
M_t , M_s , M_m	EMA rod, equivalent flight surface and equivalent motor mass	[*Kg*]
p	Lead of roller screw	[*mm*]
T_r , T_m , T_e , T_{lim}	EMA reference, output, electromagnetic and limit torque	[*Nm*]
t_s , t_{su} , t_{ss}	Ideal minimum, unsaturated and saturated response time	[*s*]
U_s , U_m	Supplied DC and motor voltage	[*V*]
V_e , V_{ex}	EMA output and aerodynamic linear velocity	[*m/s*]
x_c , x_e , x_s	EMA command, rod and flight surface position	[*m*]
α_ω , α_T	EMA rotation speed and torque saturation ratio	[-]
ε_p , ε_d	Static position and static disturbance tracking error	[*m*]
σ_p , σ_{pu} , σ_{ps}	Ideal unsaturated and saturated overshoot	[-]
ω_r , ω_m , ω_{lim}	Motor reference, actual and limit velocity	[*rad/s*]
ω_n	Natural frequency	[*rad/s*]
ξ	Damping factor	[-]

BLDC, PMSM	Brushless Direct Current and Permanent Magnet Synchronous Motor
SHA, EHA, EMA	Servo-Hydraulic, Electro-Hydrostatic and Electromechanical Actuator
LVDT	Linear Variable Displacement Transducer
PDE	Power Drive Electronics

1 INTRODUCTION

As the rapid growth of air traffic market in recent years, man-made CO_2 emissions into the atmosphere increased largely by civil aviation. The aircraft industry has to face both economic and environmental issues [1]. Currently, an interim and attractive solution is towards "More Electric Aircraft" (MEA) using more electric power technological advancements for non-propulsive systems of aircrafts. This is a key step for the ultimate goal to achieve the All Electric Aircraft (AEA) [2, 3], as far as to reduce aircraft weight and fuel consumption. Therefore, for next-generation airplanes, electrical power networks in place of the conventional hydraulic, pneumatic and mechanical ones are an inexorable trend. On this basis, today's aircraft actuation systems prefer power-by-wire (PBW) and have centered on novel approaches to design and develop electrical power actuators, such as electro-hydrostatic actuator (EHA) and electromechanical actuator (EMA).

Last decades, numbers of investigations explored EHAs technologies and achieved deep understanding studies in aerospace industry. The EHAs are already implemented in latest Airbus A380 and A350 airplanes as backup for primary flight controls. However, EHAs remove only the central hydraulic power distribution, but interval use of hydraulic in the actuator. EMAs compared to EHAs, eliminate all the hydraulic circuits, as show the successful applications in Boeing 787 for secondary flight controls [4]. The use of EMAs is pursued not only because of its clean energy but also for fuel consumption reduction (because of lower weight) and maintenance cost reduction for aircraft actuation systems [5]. Hence, EMAs technologies are crucial for the concept of All Electric Aircraft. Nevertheless, nowadays in aircraft flight control field, the maturity level of EMAs technology is far behind that of conventional hydraulic actuators. One big challenge in EMAs is jamming as result of numerous linkage mechanisms. Thus at present stage for the aircraft safety, introducing redundant path or clutch devices is indispensable, but in this way, it will increase extra weight and occupy more installation space [6]. This is an undesired result and incompatible solution for aircraft actuation system design and development. Therefore, weight saving and size limit for EMA's design on basis of not to influence dynamic performances and reliability.

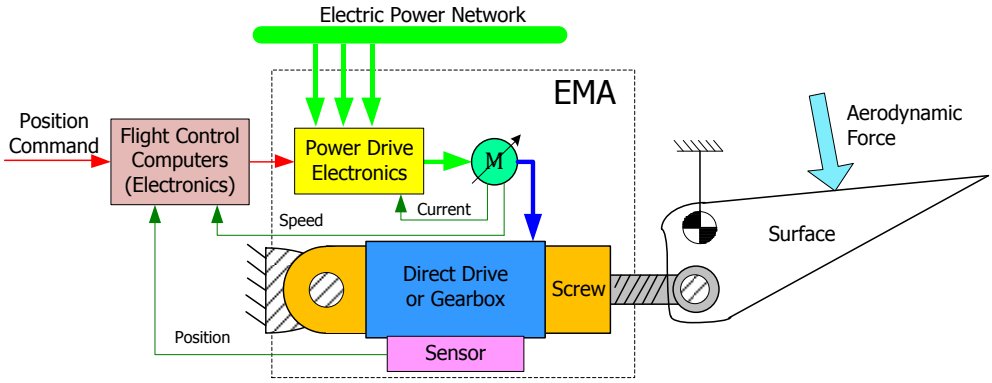

Figure 1: Overview of an EMA flight control actuation system

Currently, two types of linear EMAs are regarded for flight control applications: geared and direct drive. As shown in Figure 1, in the case of the nut screw directly connect to the rotor of motor for a whole integration, this architecture is direct drive. When the motor and mechanical transmission are separated, the mechanical power is through a gearbox then to a nut screw mechanism, this architecture is geared EMA. Whichever type of EMAs, the electric energy is converted into mechanical one by a rotary electric motor which transfers the mechanic power to the control surface through a gearbox and/or nut-screw mechanism. Direct drive EMAs cancel the gear reduction and offer a high potential for geometrical

integration of the nut-screw reducer and the electric motor. This concept may be lighter and more compact, and thus more suitable and competitive for aerospace applications.

The illustrative example used in this communication is a linear direct drive aileron actuator. First, are explained the dynamic performances (stability, settling time and first overshoot) under the assumption of a linear model of EMA. Since multiloop control architecture is mostly used for the control of such systems, linear control theory shows that any desired dynamics can be achieved by the controlled system (refer to section 3 for the demonstration). However, owing to the above-mentioned constraints, the EMA operates in conditions that are not captured by the linear model used for controller design. For instance, since the airframe is designed to be as light as possible, the actuator anchorage compliance is not negligible. Since the driven load inertia and the force disturbances are important, the compliances of the EMA's nut screw may become a critical parameter. In these conditions, the coupling between the structural and the actuator dynamics alters the performance of the whole actuation function that can even become unstable. As the actuator is also subjected to mass and volume constraints, the motor rated torque has to be minimized. Consequently, this limit introduces a saturation effect between the demanded and the produced electromagnetic torque. Thus, these technological limitations/imperfections make the real performance far different from the performance expected when a liner model is used for control design. Moreover, since the control becomes a constrained problem, some performance requirements may be even unreachable. In these conditions the controller will have to "live" with these limitations and still ensure the required performance.

This communication is organized in 6 sections. Section 1 introduces the study objective and contribution of this paper. Section 2 descripts the considered EMA consist, then establishes its linear mathematical model and presents classic control structure. In section 3, the system performance requirements are introduced. Section 4 analyzes the saturation effects and shows some simulation results. Section 5 discusses the compliances effects and presents the results of simulations. Finally, conclusions are drawn in section 6.

2 EMA SYSTEM DESCRIPTION

An equivalent linear EMA system with the conventional cascade control architecture is illustrated in Figure 2: Here can be identified the current loop (inner loop), speed loop (middle loop) and position loop (outer loop). The control system gets position reference from the pilot/autopilot and calculates the duty cycle for the power electronics in order to meet the EMA dynamic performance requirements.

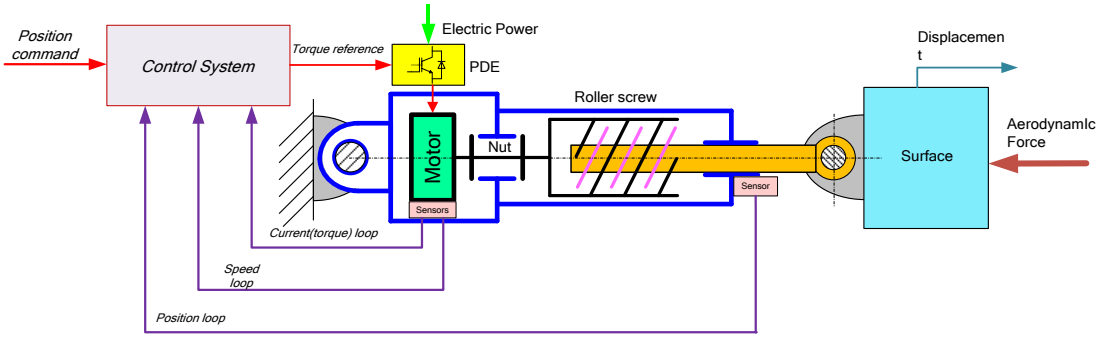

Figure 2: Multiloop control structure for a direct drive linear EMA system

2.1 Basic Structure

In this communication it is considered that a direct drive linear EMA has the following components:

- A control system for position control
- An electric motor (DC type or 3-phases BLDC, PMSM)
- A power drive electronic
- A current sensor, a speed resolver and a LVDT
- A roller-screw transmission mechanism
- A flight surface.

2.2 Simplifications and Assumptions

In this paper, the considered dynamic performances of the EMA system are the stability the settling time and the first overshot. Usually, the controller design is based on a liner model of the system, which is most often of low order. However, technological limitations such as torque/velocity saturation render the model nonlinear while the presence of the compliance increases its order. We will study separately the impact of these two effects. Therefore, three models will be used along the paper: a low order model without saturations and compliance in order to express the expected dynamics when the controller is designed; a simulation model that adds saturations to the former model; and finally the third one modeling the effect of the compliance (but without the effect of the saturations). Along the three presented modeling stages, some simplifications and assumptions are considered:

- The bandwidth of the PDE and the current loop of the motor are much higher (typically 500Hz-1KHz) as compared to the other two, so it can be neglected in our study.
- For the first two models, the anchorage, the joint between the motor and the roller-screw and the EMA rod are considered perfectly rigid.
- The motor and roller-screw inertia are merged in a single lumped inertia, while the rod mass is neglected.
- The friction effects are neglected (corresponding to the worst case, affects system stability) [7].
- The backlash and preload in the EMA kinematics are neglected.
- The power limitations and saturations are neglected in the third modeling.
- The digital signal effects (delay, sampling, quantizing, etc.) are neglected.

2.3 Linear Virtual Prototype

The schematic of EMA functional architecture with its control system is shown in Figure 3. We can identify all the three control loops. However, when the current loop is ignored, the input of the motor (actually its mechanical part) becomes the electromagnetic torque T_e. If torque saturation of the motor is not considered, the electromagnetic torque T_e is equal to the command of the velocity loop T_r.

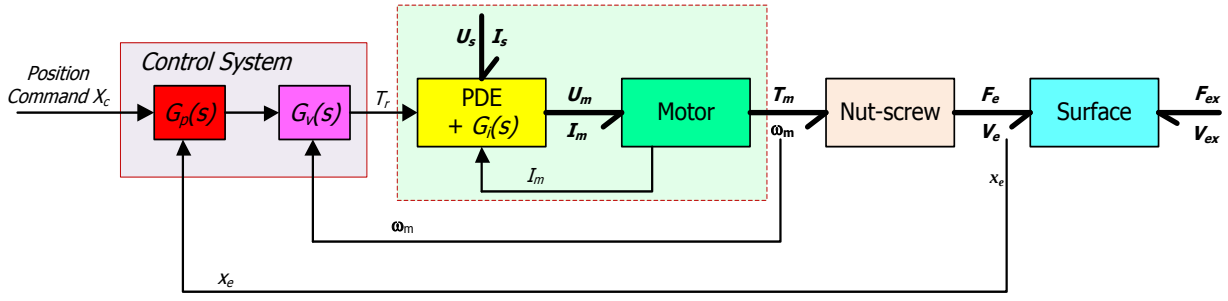

Figure 3: Block diagram of EMA linear prototype architecture

For the mathematical modeling of the controlled system we can develop the following physical equations. The torque balance at the motor shaft is:

$$T_e = T_m + J_m \dot{\omega}_m \tag{1}$$

The mechanical power transferred from rotational motion into translational one through the nut-screw is:

$$\begin{cases} V_e = \dfrac{p}{2\pi}\omega_m \\ F_e = \dfrac{2\pi}{p}T_m \end{cases} \tag{2}$$

The surface dynamics equation can be expressed as:

$$F_e - F_{ex} = M_s \ddot{x}_s \tag{3}$$

For small angular displacements of the surface (aileron), it can be assumed that:

$$X_s = X_e \tag{4}$$

Applying Laplace transform to the upper equations (1) to (3), the displacement X_s can be expressed as:

$$X_s(s) = \frac{\dfrac{2\pi}{p}T_r(s) - F_{ex}(s)}{\left(M_s + \dfrac{4\pi^2}{p^2}J_m\right)s^2} \tag{5}$$

It is worth mentioning that equation (5) shows that even a small motor inertia will reflect a huge equivalent mass (because p is very small) at the EMA rod level, which strongly affects the system dynamic performances:

$$M_m = \frac{4\pi^2}{p^2}J_m \tag{6}$$

$$J_s = \left(\frac{p}{2\pi}\right)^2 M_s \tag{7}$$

Also equation (6) shows that the open loop of the EMA linear model is a second order system, with one pair of pure imaginary poles. The absence of the damping is explained by the deliberate omission of the viscous friction, which corresponds to the worst case scenario.

2.4 Controller Design

On the basis of the EMA open loop linear model analysis, for a no damping and poor natural dynamics, a simple proportional position controller cannot meet the closed-loop requirements. One of the common ways get around this problem is to design a proportional derivative (PD) position controller and/or to introduce a speed loop. Comparing these two approaches for controller design, the latter has the clear advantages of:

- Using the actual rotor speed

- No need to derivate the input position command signal, thus reducing sampling errors
- No derivation of the measurement noise
- Easy to separate anticipation and stabilization regulators.

A position and speed feedback will be used for EMA control. The position gain is K_p [*Nm/m*] and the speed gain is K_v [*Nm/(rd/s)*]. The block diagram of the closed-loop EMA system is displayed in Figure 4.

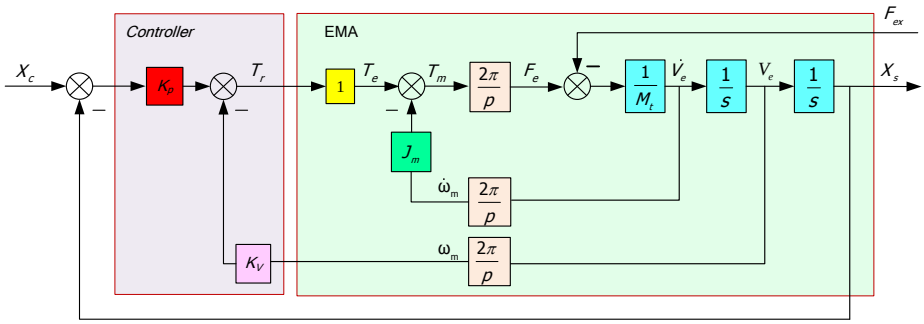

Figure 4: Block diagram of the EMA control (linear model)

Note that on the upper EMA linear model block diagram, the speed gain K_v has the same effect as the system viscous friction coefficient. Since the latter is not always known during the preliminary design stage, the speed gain adjustment can be considered as alternative procedure for system level friction modeling.

The position controlled closed-loop transfer function of EMA linear model can be expressed as following:

$$X_s(s) = \frac{X_c(s) - \frac{p}{2\pi K_p} F_{ex}(s)}{\frac{1}{K_p}\left(\frac{pM_s}{2\pi} + \frac{2\pi J_m}{p}\right)s^2 + \frac{2\pi K_v}{pK_p}s + 1} \tag{8}$$

3 PERFORMANCE REQUIREMENTS OF THE SYSTEM

Generally, the regarded performance requirements for closed-loop control systems are mainly:

- Stability
- Rapidity
- Accuracy for position pursuit and load rejection tracking error.

For second order systems, the dynamic performances are completely characterized by two parameters: the damping ratio ξ and the natural frequency ω_0, which in our case can be expressed as:

$$\begin{cases} \xi = \dfrac{K_v}{\sqrt{K_p}} \dfrac{1}{\sqrt{\dfrac{p^3}{2\pi^3}(M_s + M_m)}} \\ \omega_n = \dfrac{\sqrt{K_p}}{\sqrt{\dfrac{p}{2\pi}(M_s + M_m)}} \end{cases} \tag{9}$$

For a set of required dynamic performances, imposed by the parameters $\hat{\xi}$ and $\hat{\omega}_n$, the control parameters K_p and K_v, can be obtained from equation (9)-(11) as:

$$\begin{cases} K_p = \hat{\omega}_n^2 \dfrac{p}{2\pi}(M_s + M_m) \\ K_v = 2\hat{\xi}\hat{\omega}_n (\dfrac{p}{2\pi})^2 (M_s + M_m) \end{cases} \tag{10}$$

When for second order systems the damping ratio equals 0.707, the system is stable with an overshoot of 5%. So an ideal minimal response time t_s calculated as:

$$if \quad \hat{\xi} = 0.707 \Rightarrow t_s = \frac{2.9}{\hat{\omega}_n} \tag{11}$$

Moreover, because of the pure integrator in the direct loop, the system static tracking error for a step set-point is zero. By substituting equation (12) into (9), the static disturbance error for load rejection can be expressed as:

$$\varepsilon_d = \frac{p}{2\pi K_p} F_{ex} \tag{12}$$

Therefore, for the disturbance input, with the low-frequency closed-loop of EMA linear model has an equivalent stiffness of:

$$k_e = \frac{2\pi K_p}{p} \tag{13}$$

Thus, analyzing the upper results, it can be concluded that the system can achieve any required dynamic performance. However, we can imagine that in the presence of power limitations and technologic imperfections it is not possible to attain any required performance.

4 SATURATION EFFECTS

Maximal power is always a design parameter for EMA. Maximum voltage limit impacts the maximal motor speed while maximum current impacts the maximal motor torque. These saturations can be modeled as shown in Figure 5.

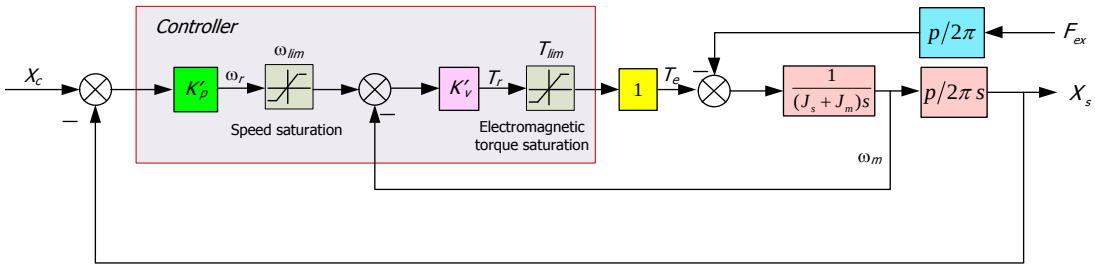

Figure 5: Cascade controller considering torque and velocity saturations for EMA

Note that these two saturations will not alter the stability of the system (if the unsaturated system is designed to be stable), which aims to identify and quantify the impact of the speed and torque saturation of the control EMA in order to take into account during the preliminary design.

Compared to the equation (12), the numerical expressions of controller gains can be written as:

$$\begin{cases} K_p^{'} = \dfrac{K_p}{K_v} = \dfrac{\pi\hat{\omega}_n}{p\hat{\xi}} \\ K_v^{'} = K_v = 2\hat{\xi}\hat{\omega}_n(\dfrac{p}{2\pi})^2(M_s + M_m) \end{cases} \tag{14}$$

In the position-controlled, when the set-point amplitude is X_c and the control system is unsaturated, the speed and torque reference are givens as:

$$\begin{cases} \omega_r = K_p^{'}(x_c - x_s) \\ T_r = [K_p^{'}(x_c - x_s) - \omega_m]K_v^{'} \end{cases} \tag{15}$$

Thus we can estimate that the maximal values of these references are:

$$\begin{cases} \omega_{rmax} = K_p^{'}x_c \\ T_{rmax} = K_p^{'}K_v^{'}x_c \end{cases} \tag{16}$$

In order to evaluate the influence of these nonlinearities on the dynamic performance we can define the speed saturation ratio and torque saturation ratio as:

$$\alpha_\omega = \frac{\omega_{lim}}{\omega_{rmax}} \in [0,\ 100\%] \tag{17}$$

$$\alpha_T = \frac{T_{lim}}{T_{rmax}} \in [0,\ 100\%] \tag{18}$$

Multiple simulations of the saturated model from Figure 5 are carried out in MATLAB/Simulink, from above equations, as known that the system response time is a function of position controller gain and EMA lead of nut-screw, the equivalent motor mass does not affect the response time, but requires the speed controller gain to be adjusted.

Firstly, a simulation work is aimed to a specific surface mass (600 kg) and screw lead (2.54 mm) in EMA system but varying the desired response time t_s in 5 typical levels: 0.01s, 0.05s, 0.1s, 0.5s, and 1s, meanwhile change the equivalent motor mass from 1 to 100 times bigger than surface mass. The simulation results presented in Table 1, it shows that the change motor equivalent mass (variable motor inertia) for EMA design has nearly no influence on the performance degradation for any response time desire but needs to the speed controller to be adjusted at the same time. Therefore using a specific motor mass for following study saturation effects is available.

Table 1: Ratio of response time obtained and response time desire T_{su}/T_s

T_s (s)	Ratio of the equivalent motor mass and surface mass: M_m/M_s										
	1	10	20	30	40	50	60	70	80	90	100
0.01	1.0011	1.0011	1.0011	1.0011	1.0011	1.0011	1.0011	1.0011	1.0011	1.0011	1.0011
0.05	1.001	1.001	1.001	1.001	1.001	1.001	1.001	1.001	1.001	1.001	1.001
0.1	1.0008	1.0008	1.0008	1.0008	1.0008	1.0008	1.0008	1.0008	1.0008	1.0008	1.0008
0.5	1.0004	1.0004	1.0004	1.0004	1.0004	1.0004	1.0004	1.0004	1.0004	1.0004	1.0004
1	1.0003	1.0003	1.0003	1.0003	1.0003	1.0003	1.0003	1.0003	1.0003	1.0003	1.0003

Then in next, the torque or speed saturation ratios were varied. For each value of the saturation ratio, different values of inertia, lead of the nut-screw and required closed-loop natural frequency where tested as well. The obtained results were used to trace the degradation of the response time (in Figure 6) and first overshoot (in Figure 7) as a function of the speed saturation and torque saturations. It turns out that inertia, nut-screw lead and the closed-loop natural frequency do not have any impact on the curves presented in Figure 6 and 7 (K'_p and K'_v are automatically recalculated for the new set of parameters). On the abscise, 10% means that the saturation T_{lim} represents a tenth of the maximal unsaturated command while 100% means that there is no saturation. The same holds for the speed saturation.

The simulation results of Figures 6 and 7 show that lower percentage speed saturation has stronger effect for system response time. A 20% speed saturation ratio will increase by 3 times the response time comparing to the desired one obtained without saturation. However, it improves system stability by reducing system overshot. Regarding the torque saturation, it impacts considerably the response time when it gets below 15%. Its effect is very strong, on both the response time and the overshot.

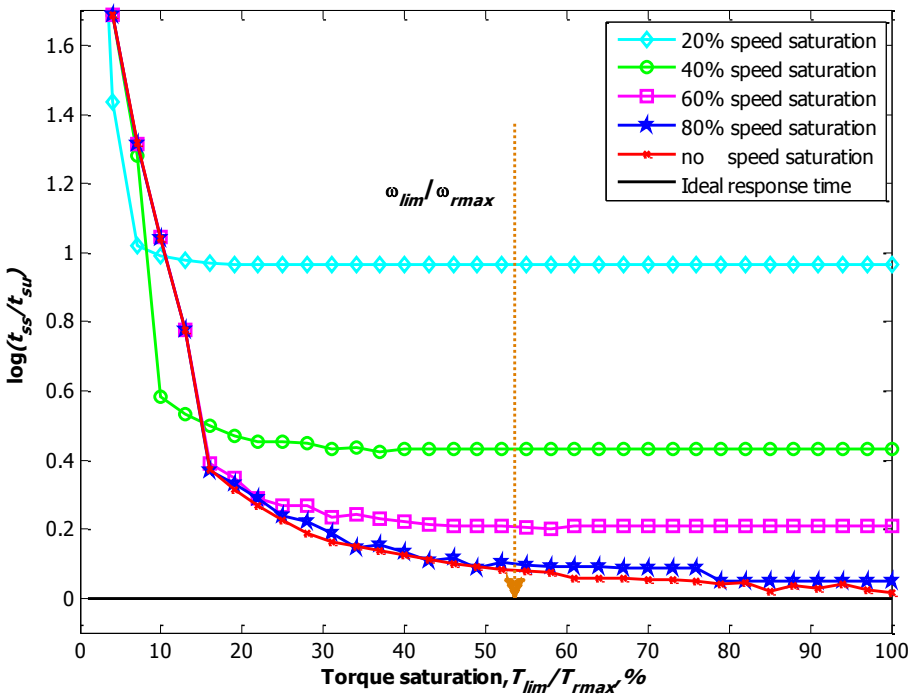

Figure 6: Dimensionless response time depending on torque and speed saturation

Thus these curves can be used to extract some best practice rules to be used during preliminary design of EMA, such as: for a given set of dynamic performance and system parameters, The torque saturations of about 25-30% and speed saturation of 60% can be accepted. The cited values are given only as an illustrative example if for instance a response time degradation of 50% is tolerated.

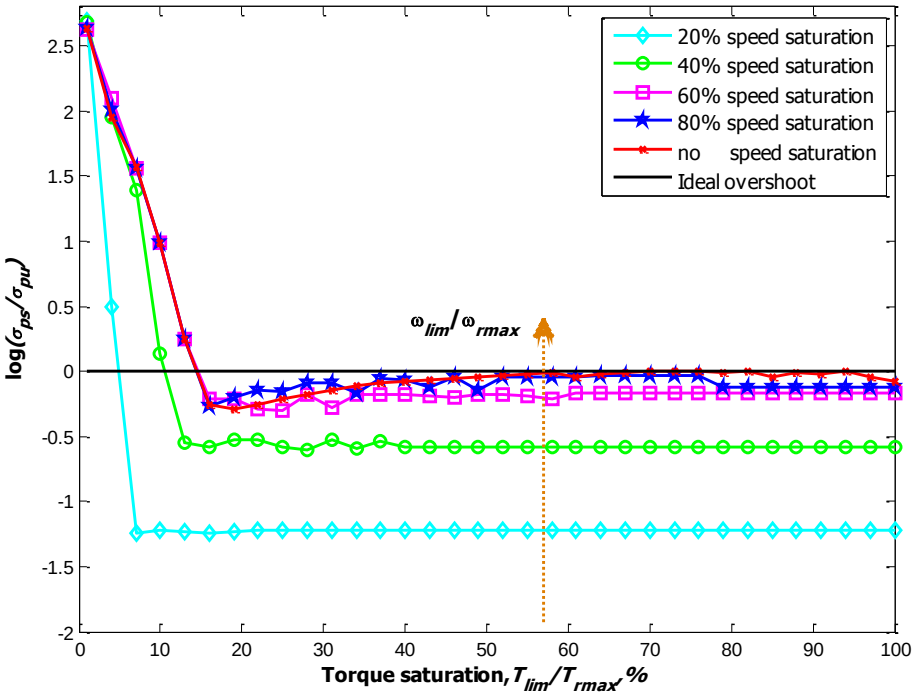

Figure 7: Dimensionless first overshoot depending on torque and speed saturation

5 COMPLIANCE EFFECTS

Most of the analysis and research work on EMA systems uses a rigid model where the actuator is rigidly attached between the main structure and the load. However, due to the harsh environment and trend of integrated design, the compliance may become important and alter the system stability [8]. A structural diagram of EMA is described in Figure 8. Generally, it can be identified the anchorage (k_a) and transmission (k_t) stiffness coming from the aircraft structure, and the stiffness of the EMA nut-screw mechanism (k_s).

In order to consider the worst case of control system stability, the structural damping coefficients are assumed to be negligible. In these conditions some oscillations of the control surface and the EMA appear from the combination of mass (M_m, M_t and M_s) and compliance (k_a, k_s and k_t). In practice, the actuator body and rod masses are very small compared to the equivalent motor inertia (see relation (6)), so they can be neglected. To simplify the analysis, the anchorage and transmission stiffness can be considered in series connection which gives a single structural stiffness (k_z), expressed as:

$$k_z = \frac{k_a k_t}{k_a + k_t} \tag{18}$$

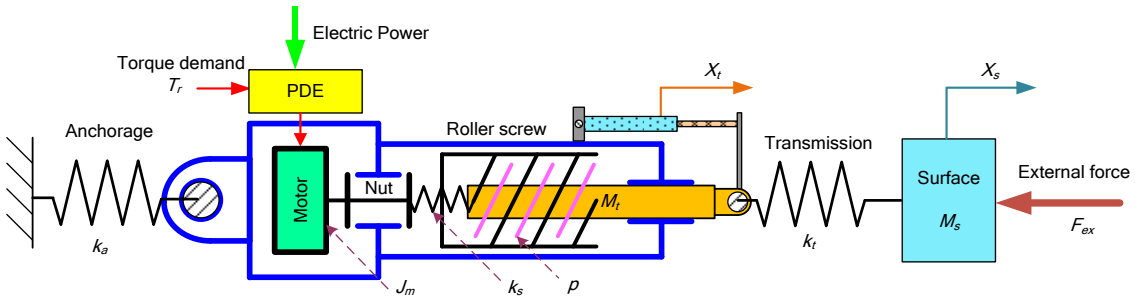

Figure 8: EMA configuration with structural compliances

The considered control structure in this case is still cascade control but the effect of the torque and speed saturations are not considered here. The equivalent schematic diagram with the controller is shown in Figure 8. Considering a realistic integration of the position sensor, the position feedback is obtained at the EMA rod level (X_t) and not at the control surface level (X_s). Ignoring the rod mass, the order of system transfer function is 4. The closed-loop transfer function for set-point tracking (F_{ex} = 0) is:

$$\frac{X_t(s)}{X_c(s)} = \frac{2\pi p \frac{k_s k_z}{k_s + k_z} K_p (\frac{M_s}{k_t} s^2 + 1)}{p^2 M_m M_s s^4 + 4\pi^2 M_s K_v s^3 + [p^2 \frac{k_s k_z}{k_s + k_z}(M_m + M_c) + 2\pi p M_s \frac{k_s}{k_s + k_z} K_p] s^2 + 4\pi^2 \frac{k_s k_z}{k_s + k_z} K_v s + 2\pi p \frac{k_s k_z}{k_s + k_z} K_p} \tag{19}$$

The control surface position when considering the transmission compliances effects, can be expressed as:

$$X_s(s) = \frac{k_z}{M_s s^2 + k_z} X_c(s) \tag{20}$$

The characteristic equation of the closed loop system becomes:

$$D(s) = p^2 M_m M_s s^4 + 4\pi^2 M_s K_v s^3 + [p^2 \frac{k_s k_z}{k_s + k_z}(M_m + M_c) + 2\pi p M_s \frac{k_s}{k_s + k_z} K_p] s^2 + 4\pi^2 \frac{k_s k_z}{k_s + k_z} K_v s + 2\pi p \frac{k_s k_z}{k_s + k_z} K_p \tag{21}$$

and closed-loop transfer function of load rejection (X_c = 0) at the road level is:

$$\frac{X_t(s)}{F_{ex}(s)} = \frac{p^2 M_m \frac{k_z}{k_s + k_z} s^2 + 4\pi^2 K_v \frac{k_z}{k_s + k_z} s + p^2 \frac{k_s k_z}{k_s + k_z}}{D(s)} \tag{22}$$

The closed-loop compliance transfer function of the surface control level is:

$$\frac{X_s(s)}{F_{ex}(s)} = \frac{p^2 M_m s^2 + 4\pi^2 K_v s + p^2 \frac{k_s k_z}{k_s + k_z} + 2\pi p \frac{k_s}{k_s + k_t} K_p}{D(s)} \tag{23}$$

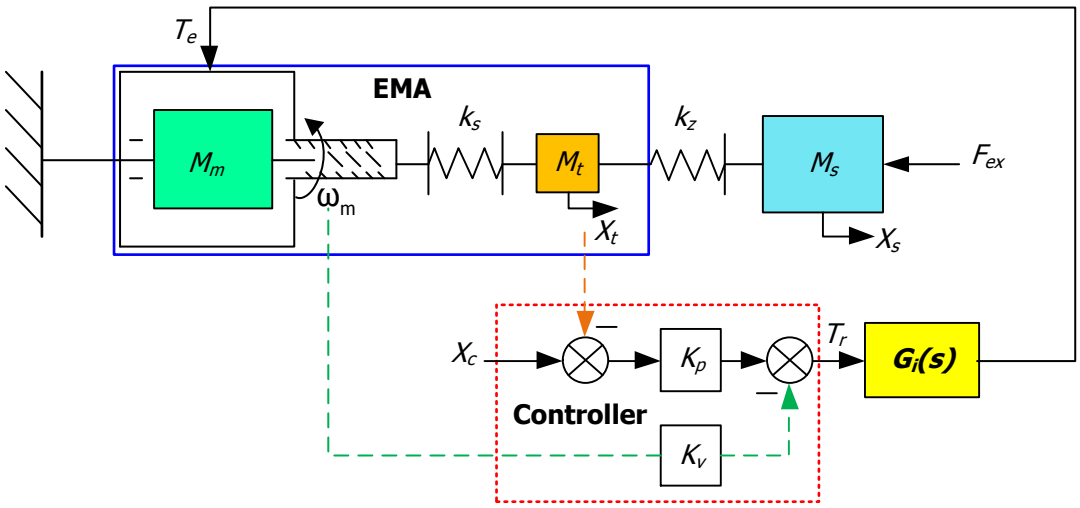

Figure 9: Equivalent schematic of position controlled EMA with compliances

The first studied effect of the compliance is the verification of system stability. For a fourth-order model, eq. (23), the appropriated method to study stability is to use the Routh Stability Criterion [9]. The obtained criterion for stability is:

$$k_s > \frac{2\pi}{p} K_p \Leftrightarrow k_s > \hat{\omega}_n^2 (M_s + M_m) \tag{24}$$

Equation (24) indicates that the system stability depends only on the position gain of the controller. Since the latter depends on the system equivalent mass and desired dynamics, we get another good practice rule for preliminary design. In order to reach a desire control performance (response time), the compliance should satisfy the constraint from eq. (24).

When considering compliance effects, from equation (24) for disturbance rejection. The static position error under external load is:

$$\varepsilon_d = \left(\frac{p}{2\pi K_p} + \frac{1}{k_t}\right) F_{ex} \tag{25}$$

Comparing equations (25) and (13), it shows that the structural compliance will reduce the closed loop system stiffness and increase the static disturbance. A simulation of position performance, comparing without and with compliance is given in Figure 11. A linear position step command X_c = 10 mm for flight surface is applied at t = 0.1s, which is followed by a 10 KN external aerodynamic force step occurring at t = 1.5s (disturbance). The controller was designed to get a desired response time T_s = 0.05s and a first overshoot of σ_p < 5%. Note that set-point tracking and disturbance rejection dynamics are very different: In the presence of compliance the surface displacement has a big oscillation amplitude with a frequency about 35 Hz, the realistic response time is 0.3s, which is 6 times longer than that of the ideal second-order without compliance effect. Because of the transmission compliance the static disturbance impact is also bigger.

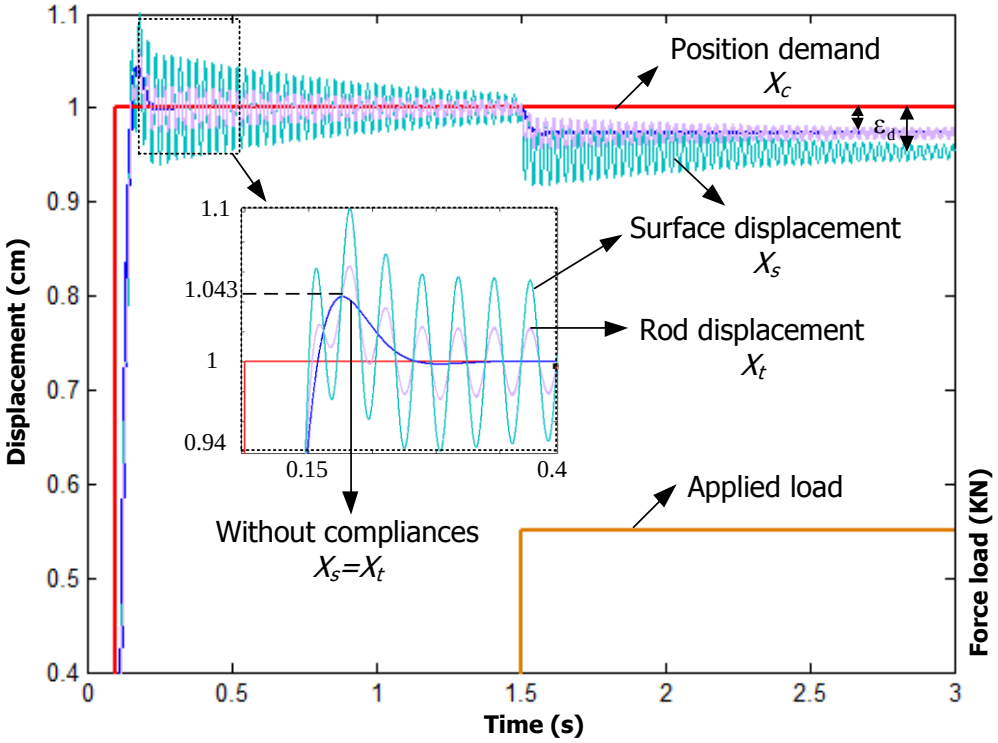

Figure 10: Position pursuit and rejection considering compliances

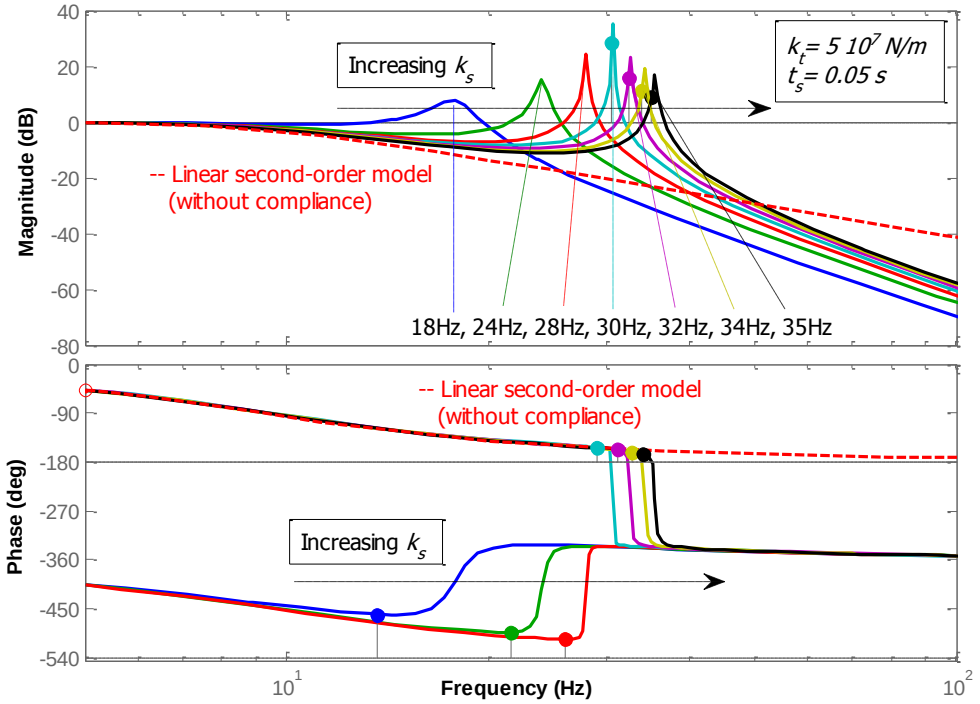

Figure 11: Bode diagram of surface position tracking with compliance effects

The frequency response of the surface displacement with respect to the position set-point can be simulated, and the results are shown in Figure 11. The ideal linear second-order EMA model without compliance is compared with the models of various compliances. The practical transmission compliance k_t is set to 5×10^7 N/m, we change the EMA mechanism compliance k_s in a ratio of 7 (from 1×10^7 to 7×10^7 N/m) to vary the global system compliance but with the same controller design. By application of a trajectory for response time 0.05s that is surface frequency in 9Hz according to eq. (11). In Figure 11, which shows that firstly there is no resonant peak for linear second-order model (red dashed), and it is stable in this case of controller design. However, during k_s increasing (from small to huge design), the stability of models considering compliances is varying from unstable (first 3 curves) to stable (latest 4). This verifies the system stability rule in eq. (24). Even though designed an infinite EMA compliance, which only can eliminate the EMA rod resonance but not the surface resonance peak, because it exists realistic transmission compliance. Therefore, the compliances effects in EMA system are cross-linked, which affects the component design and whole system dynamic performances.

6 CONCLUSION

In the presence of saturations and compliance it is important to make available generic preliminary design rules for electro-mechanical position actuation system. Mechanical engineers can use these relations as "best practice rules" [10] for the specification and preliminary design of the mechanical part, enabling the dynamic performance requirements to be met in practice. Control engineers may use these design rules to reduce the number of design iterations through rapid verification of consistency between closed-loop performance requirements and early choices and definition of the mechanical components. It has been shown that the performance reduction becomes significant when the torque and speed saturations decrease to about 15% of the unsaturated model. Also, because of structural stiffness, the surface and rod displacement is not the same and may enter in resonance. To prevent this, easier the control performance should be revised, easier the mechanical parts should be chosen consecutively.

REFERENCES

[1] X. Roboam, B. Sareni, and A. D. Andrade, "More electricity in the air: Toward optimized electrical networks embedded in more-electrical aircraft," *Industrial Electronics Magazine, IEEE,* vol. 6, pp. 6-17, 2012.

[2] S. L. Botten, C. R. Whitley, and A. D. King, "Flight control actuation technology for next-generation all-electric aircraft," *Technology Review Journal,* vol. 8, pp. 55-68, 2000.

[3] W. Cao, B. C. Mecrow, G. J. Atkinson, J. W. Bennett, and D. J. Atkinson, "Overview of electric motor technologies used for more electric aircraft (MEA)," *Industrial Electronics, IEEE Transactions on,* vol. 59, pp. 3523-3531, 2012.

[4] J. Rosero, J. Ortega, E. Aldabas, and L. Romeral, "Moving towards a more electric aircraft," *Aerospace and Electronic Systems Magazine, IEEE,* vol. 22, pp. 3-9, 2007.

[5] M. Villani, M. Tursini, G. Fabri, and L. Castellini, "High reliability permanent magnet brushless motor drive for aircraft application," *Industrial Electronics, IEEE Transactions on,* vol. 59, pp. 2073-2081, 2012.

[6] M. Todeschi, "Airbus-EMAs for flight controls actuation system-perspectives," in *Recent Advances in Aerospace Actuation Systems and Components*, Toulouse, 2010, pp. 1-8.

[7] J.-C. Maré, "Friction modelling and simulation at system level: a practical view for the designer," *Proceedings of the Institution of Mechanical Engineers, Part I: Journal of Systems and Control Engineering,* pp. 728-741, 2012.

[8] J.-C. Maré, "Electro hydraulic force generator for the certification of a thrust vector actuator," in *Recent Advances in Aerospace Actuation Systems and Components*, Toulouse, 2001, pp. 59-64.

[9] F. Golnaraghi and B. Kuo, *Automatic control systems* vol. 2, 2010.

[10] J.-C. Maré, "Best practices in system - level virtual prototyping - application to mechanical transmission in electromechanical actuators " in *5th International Workshop on Aircraft System Technologies*, Hamburg, 2015.